HERIOT WATT UNIVERSITY

Heriot-Watt University
Research Gateway

Sonic black hole horizon formation for Bose-Einstein condensates with higher-order nonlinear effects

Citation for published version:
Yang, Y, Wang, Y, Zhao, L, Song, D, Zhou, Q & Wang, W 2019, 'Sonic black hole horizon formation for Bose-Einstein condensates with higher-order nonlinear effects', *AIP Advances*, vol. 9, no. 11, 115203. https://doi.org/10.1063/1.5124934

Digital Object Identifier (DOI):
10.1063/1.5124934

Link:
Link to publication record in Heriot-Watt Research Portal

Document Version:
Publisher's PDF, also known as Version of record

Published In:
AIP Advances

Publisher Rights Statement:
© 2019 Author(s).

General rights
Copyright for the publications made accessible via Heriot-Watt Research Portal is retained by the author(s) and / or other copyright owners and it is a condition of accessing these publications that users recognise and abide by the legal requirements associated with these rights.

Take down policy
Heriot-Watt University has made every reasonable effort to ensure that the content in Heriot-Watt Research Portal complies with UK legislation. If you believe that the public display of this file breaches copyright please contact open.access@hw.ac.uk providing details, and we will remove access to the work immediately and investigate your claim.

Download date: 25. Mar. 2025

AIP Advances

Sonic black hole horizon formation for Bose-Einstein condensates with higher-order nonlinear effects

Cite as: AIP Advances **9**, 115203 (2019); https://doi.org/10.1063/1.5124934
Submitted: 18 August 2019 . Accepted: 18 October 2019 . Published Online: 12 November 2019

Yang Yang, Ying Wang, Li Zhao, Dongpo Song, Qingchun Zhou, and Wei Wang

View Online Export Citation CrossMark

ARTICLES YOU MAY BE INTERESTED IN

What has the Rosetta probe taught us about comet tails?
Scilight **2019**, 441102 (2019); https://doi.org/10.1063/10.0000197

X-ray spectroscopy evidence for plasma shell formation in experiments modeling accretion columns in young stars
Matter and Radiation at Extremes **4**, 064402 (2019); https://doi.org/10.1063/1.5124350

Melting curve of vanadium up to 470 GPa simulated by ab initio molecular dynamics
Journal of Applied Physics **126**, 205901 (2019); https://doi.org/10.1063/1.5124520

NEW AVS Quantum Science
A high impact interdisciplinary journal for ALL quantum science
ACCEPTING SUBMISSIONS

AIP Publishing

© 2019 Author(s).

Sonic black hole horizon formation for Bose-Einstein condensates with higher-order nonlinear effects

Cite as: AIP Advances 9, 115203 (2019); doi: 10.1063/1.5124934
Submitted: 18 August 2019 • Accepted: 18 October 2019 •
Published Online: 12 November 2019

View Online Export Citation CrossMark

Yang Yang,[1,2] Ying Wang,[1,2,a)] Li Zhao,[3] Dongpo Song,[1] Qingchun Zhou,[2] and Wei Wang[2,4,b)]

AFFILIATIONS

[1]School of Science, Jiangsu University of Science and Technology, Zhenjiang 212003, China
[2]Laboratory of Advanced Optics, Jiangsu University of Science and Technology, Zhenjiang 212003, China
[3]School of Materials Science and Engineering, Jiangsu University of Science and Technology, Zhenjiang 212003, China
[4]School of Engineering and Physical Sciences, Institute of Photonics and Quantum Sciences, Heriot-Watt University, Edinburgh EH14 4AS, United Kingdom

[a)]wangying@just.edu.cn
[b)]w.wang@hw.ac.uk

ABSTRACT

We study sonic horizon formation dynamics for Bose-Einstein condensate systems with higher-order nonlinear interaction. Based on the Gross-Pitaevskii equation incorporating higher-order nonlinear effects and through a variational method, we derived the criteria formula for sonic horizon occurrence. The key features of the sonic horizon are pictorially demonstrated, and we identified the stabilization and widening metastable effects of the higher-order nonlinear interaction, from which the quantitative results can be used to guide relevant experimental observations of sonic black holes with higher-order nonlinear effects.

© 2019 Author(s). All article content, except where otherwise noted, is licensed under a Creative Commons Attribution (CC BY) license (http://creativecommons.org/licenses/by/4.0/). https://doi.org/10.1063/1.5124934

I. INTRODUCTION

The study of nonlinear phenomena is a fascinating subject in the physical sciences. Phenomena exhibiting typical nonlinear behaviors such as solitons and vortices have heavily been investigated both experimentally and theoretically.[1–6] Ultracold atomic systems are the ideal choice for studying many intriguing nonlinear dynamical problems because of their flexible controllability and ease with which the experimental setting can be modulated. One category of interesting nonlinear problems that has attracted the attention of physicists in ultracold system manipulation is sonic black hole evolution, which comes into play by the formation of a sonic horizon. Originally, black hole phenomena are problems closely scrutinized in astrophysics, but because of the uncontrollability and unrepeatability of black holes in astrophysics, some characteristic occurrences such as horizon formation and Hawking radiation are difficult to detect. However, as pointed out by Unruh, if we identify the quantum fluid flow with curved spacetime in astrophysics and the system excitation mode with the spacetime field, a sonic analog of the black hole (i.e., a sonic black hole) can be utilized to study black-hole-related problems in astrophysics.[7,8] The sonic horizon, which is the boundary between the region of fluid supersonic flow and the region of subsonic flow, just corresponds to the event horizon in astrophysics, which prevents everything, including light, from escaping from the trapped region inside the horizon. Therefore, like the event horizon in astrophysics, the investigation of the sonic horizon is crucial in the study of problems related to sonic black holes.[9,10]

The typical ultracold atomic system, such as a Bose-Einstein condensate (BEC) that supports the formation of the sonic horizon, is usually modulated through interparticle nonlinear interaction to induce horizon formation.[11–15] The system's dynamical evolution that leads to the formation of the sonic horizon also causes vast system mass density fluctuations in space and time. When the system's three-body interaction plays a significant role, the higher-order nonlinear interaction effect has to be considered.

© Author(s) 2019

Therefore, in this study, for a ground-state BEC with nonlinear interaction modulation, through the Feshbach resonance technique, for example, we study its sonic horizon formation based on the Gross-Pitaevskii equation (GPE) incorporating higher-order nonlinear terms.[16,17] Through the variational method, we derive the evolution equation for the BEC mass distribution parameters from which the criteria formula of sonic horizon occurrence is derived through the difference formula of the system flow speed and sound speed. The dynamical "potential" curve that leads to sonic horizon typical occurrence is pictorially demonstrated and compared with that where higher-order nonlinear interaction is not considered.[18,19] We identify the principal stabilization effect of the nonlinear interaction for the system oscillation mode at leading and quintic order nonlinearity, which is crucial for the occurrence of the sonic horizon. In addition, we identify that the repulsive (positive) higher-order nonlinear interaction tends to stabilize the oscillation mode of the system, while the attractive (negative) interaction tends to make the evolution mode of the sonic black hole metastable. The theoretical results obtained in this study can be used to guide relevant experimental observation of the sonic black hole horizon where higher-order nonlinear effects play a significant role.

This study is organized as follows: Sec. II presents the GPE model incorporating the higher-order nonlinear effects. Section III describes the procedural details for the derivation of the sonic horizon dynamical variables. The key features are analyzed and pictorially demonstrated in Sec. IV. Section V gives concluding remarks.

II. THE GROSS-PITAEVSKII EQUATION MODEL WITH HIGHER-ORDER NONLINEAR INTERACTIONS

As an effective model for describing the sonic black hole of Bose-Einstein condensates, the nonlinear terms of the Gross-Pitaevskii equation have significant effects on the evolution of the system. Prior work discovered the analytical formula of higher-order nonlinear interaction potential which has non-negligible effects on the system's dynamical evolution; it is[19]

$$V_{int}(r-r') = U_0[\delta(r-r') + \frac{g_2}{2}(\overleftarrow{\nabla}_r^2\delta(r-r') + \delta(r-r')\overrightarrow{\nabla}_r^2], \quad (1)$$

where $U_0 = \frac{4\pi\hbar^2 a}{m}$ is generally the hard-core interaction strength parameter. In addition, higher-order scattering effects are incorporated into the parameter $g_2 = a^2/3 - ar_e/2$ in which m, r_e, and a are the atomic mass, the effective range, and the s-scattering length, respectively. As a result, we can immediately write down the three dimensional Gross-Pitaevskii equation incorporating the higher-order nonlinear interactions as follows:

$$i\hbar\frac{\partial}{\partial t}\psi = \left[-\frac{\hbar^2}{2m}\nabla^2 + \frac{1}{2}m\Omega^2 r^2 + (g_0|\psi|^2 + g_1|\psi|^4 + g_2\nabla^2|\psi|^2)\right]\psi, \quad (2)$$

where g_0 is the chief two-body interaction strength parameter, while g_1 is the three-body interaction strength parameter and $\frac{1}{2}m\Omega^2$ is the potential strength parameter of the three dimensional isotropic harmonic trap. Our calculation for the sonic black hole horizon formation of Bose-Einstein condensates incorporating higher-order nonlinear interactions is based on the equation model (2).

III. SYSTEM OSCILLATION MODE BASED ON THE GPE MODEL INCORPORATING HIGHER-ORDER NONLINEAR INTERACTION EFFECTS

The solution of the sonic black hole formation in the Bose-Einstein condensate described by Eq. (2) is based on a modified variational approach, where the Lagrangian density of Eq. (2) takes the following form:

$$L = \psi^*\left[i\hbar\frac{\partial}{\partial t} + \frac{\hbar^2}{2m}\nabla^2 - \frac{1}{2}m\Omega^2 r^2 - \frac{1}{2}g_0|\psi|^2 - \frac{1}{3}g_1|\psi|^4 - \frac{1}{2}g_2(\nabla|\psi|)^2\right]\psi, \quad (3)$$

while the action is

$$S = \int d^3r \int dt L(r,t). \quad (4)$$

In order to investigate the evolution mode of the system in the ground state and describe the system evolution more accurately, we choose the modified wave function ansatz rather than the regular gaussian function, so the ansatz takes the following format:

$$\psi\left(\frac{r}{\rho(t)}, t\right) = \frac{C_0}{\rho^{3/2}(t)}\varphi\left(\frac{r}{\rho(t)}\right)\exp(-i\beta(t)r^2), \quad (5)$$

where C_0 is the normalization constant. Substituting Eq. (5) into Eq. (2) and solving the equation of the imaginary part, we obtain

$$\beta(t) = -\frac{m}{2\hbar}\frac{\dot{\rho}(t)}{\rho(t)}. \quad (6)$$

We can derive $L'(\dot{\rho},\rho)$ through integrating Eq. (4) with respect to space coordinates and then utilize the Euler Lagrange equation $\frac{d}{dt}\frac{\partial L'}{\partial\dot{\rho}} - \frac{\partial L'}{\partial\rho} = 0$ with respect to t, thus reaching the equation satisfied by $\rho(t)$,

$$m\ddot{\rho}(t) = -\frac{\partial V(\rho)}{\partial\rho}, \quad (7)$$

where

$$V_0(\rho) = \frac{m\Omega^2}{2}\rho^2 + \frac{\hbar^2}{2m}\frac{C_2}{C_1\rho^2}, \quad (8a)$$

$$V_1(\rho) = g_0\frac{C_3}{C_1}\frac{1}{\rho^2}, \quad (8b)$$

$$V_2(\rho) = \frac{g_1 C_4}{C_1^2}\frac{1}{\rho^4} + \frac{g_2 C_5}{C_1^2}\frac{1}{\rho^4}, \quad (8c)$$

where $V(\rho) = V_0(\rho) + V_1(\rho) + V_2(\rho)$, and

$$C_1 = \int r^2\varphi(r)^2 d^3r, \qquad C_2 = \int(\nabla\varphi)^2 d^3r,$$
$$C_3 = \int\varphi^2 d^3r, \qquad C_4 = \int\varphi^4 d^3r, \qquad C_5 = \int\varphi^2(\nabla\varphi)^2 d^3r.$$

When the nonlinear interaction strength parameters g_0, g_1, and g_2 are very small, $V \simeq V_0$. Equation (7) reduces to

$$m\ddot{\rho}(t) = -\frac{\partial V_0(\rho)}{\partial\rho}. \quad (9)$$

© Author(s) 2019

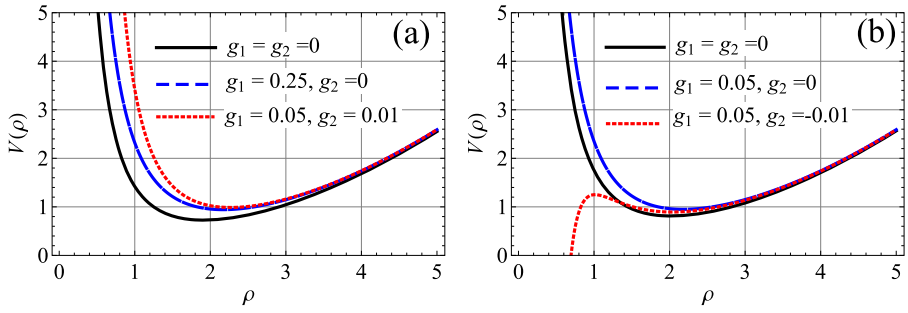

FIG. 1. Variation of "potential" $V(\rho)$ vs ρ with different orders of nonlinear interaction and sign of the highest-order nonlinear strength constant: Without incorporation of higher-order nonlinear effects (solid lines in both plots) and (a) positive g_2 and higher value of g_1 and (b) negative g_2 and smaller value of g_1.

Equation (9) can be solved strictly, with the analytical solution in the following form:

$$\rho^2(t) = A_0 \sin \omega t + B_0, \tag{10}$$

where

$$A_0 = \sqrt{\left(\frac{\rho_0^2}{2} + \frac{\hbar^2}{2m^2\Omega^2\rho_0^2}\right)^2 - \frac{C_2\hbar^2}{2C_1m^2\Omega^2}}, \tag{11a}$$

$$B_0 = \frac{\rho_0^2}{2} + \frac{C_2\hbar^2}{2C_1m^2\Omega^2\rho_0^2}, \tag{11b}$$

$$\omega = 2\Omega. \tag{11c}$$

ρ_0 is the initial distribution width of the system, from which we find that the system distribution width oscillates between the maximum value $\sqrt{B_0 + A_0}$ and the minimum value $\sqrt{B_0 - A_0}$ with frequency ω. Therefore, when the influence of nonlinear interactions g_0, g_1, and g_2 are to be taken into account, the higher-order nonlinear terms of $V(\rho)$ will affect the evolution of $\rho(t)$. For instance, when $g_0 \ll \frac{\hbar^2}{2m}\frac{C_2}{C_1}$, $|g_1| < |g_0|$, $|g_2| < |g_0|$, for (I) $g_1 = g_2 = 0$, (II) $g_1 \neq 0$, $g_2 = 0$, (III) $g_1 \neq 0$, $g_2 > 0$, and $g_1 \neq 0$, $g_2 < 0$, the graphical curves of $V(\rho)$ in the three conditions are shown pictorially in Fig. 1.

The validity of our theoretical treatment for $V(\rho)$ is based on the fact that Eq. (8a) gives the analytical relationship formula between the potential function $V(\rho)$ and ρ. The value of ρ that makes $V(\rho)$ large is not attainable actually. ρ only can take values in the range, where $E_0 - V(\rho) > 0$ (E_0 is determined by the initial system setting); suppose that ρ_0 makes $E_0 - V(\rho)$ take the maximum value and ρ_1 and ρ_2 are the roots of the equation $E_0 - V(\rho) = 0$ ($\rho_1 < \rho_0 < \rho_2$), then ρ takes the values in the range (ρ_1, ρ_2) (oscillates around ρ_0). Since when g_1 and g_2 are very small, $V(\rho) \simeq V_0(\rho)$, they only have a perturbation effect on the analytical formulation for $\rho(t)$ derived in Eqs. (9) and (10), and the actual analytical formula for $\rho(t)$ is almost the same as that shown in Eq. (10) for small nonzero g_1 and g_2.

When $\rho(t)$ varies around the minimum of the potential well $V(\rho)$ and the "total energy" is below the maximum of the $V(\rho)$ curve, $\rho(t)$ still oscillates periodically. We can see from the plots that positive higher-order nonlinear interaction plays the role of stabilizing the oscillation of $\rho(t)$ [tend to narrow the oscillation region of $\rho(t)$]. The negative higher-order nonlinear interaction constant changes oscillation motion of $\rho(t)$ to the metastable mode [when $\rho(t)$ move passing the left maximum peak of $V(\rho)$, the system suffers from instability]. Also, we identify that if the nonlinear interaction strength is not large (g_1 is small, for example), the variation of the higher-order nonlinear interaction strength will not qualitatively change the key features such as the oscillation mode, as shown by the blue curve in plots (a) and (b) of Fig. 1 with different values of quintic order (g_1) nonlinear strength.

IV. SONIC BLACK HOLE HORIZON FORMATION FROM THE OSCILLATION MODE

Based on the analytical results derived for the dynamic parameters of the system wave function in Sec. III, we can analyze the system sonic black hole horizon formation and evolution.[21] Sonic horizon formation marks the appearance of the sonic black hole. The location of the sonic horizon depends on the crossing zone of the system fluid velocity and sound velocity spatial distribution curves. The fluid velocity of the system can be derived by (5) and (6),

$$v(r,t) = \frac{\hbar}{m}\nabla(-\beta(t)r^2) = \frac{\dot{\rho}(t)}{\rho(t)}\vec{r}. \tag{12}$$

We can find that the fluid velocity of the system is isotropic and proportional to r. The conventional formula of the system sound velocity is related to $|\psi(r, t)|$, but when $g_1, g_2 \ll g_0$, the analytical form of $\varphi(r, t) \propto \psi(r, t)$ can be expressed as $\exp(-\frac{r^2}{2\rho^2(t)})$, so the sound velocity[20] of the system under this scenario is

$$c_s(r,t) \simeq \sqrt{\frac{g_0}{m}|\psi(r,t)|} \simeq \sqrt{\frac{g_0}{m}}\frac{C_0}{\rho^{3/2}(t_0)}\exp\left(-\frac{r^2}{2\rho^2(t)}\right). \tag{13}$$

The boundary location of the sonic horizon $r = r_s$ (which is of spherical shape) is determined by the solution of the following equation:

$$[v(r,t) - c_s(r,t)]|_{r=r_s} = 0. \tag{14}$$

Now, we analyze the oscillation mode of the system; $\rho(t)$ and $\dot{\rho}(t)$ are periodic functions. When g_1 and g_2 are negligibly small, the period of oscillation is derived from $T_0 = \frac{2\pi}{\omega}$ in (11c). When $\dot{\rho}(t) > 0$, the system flow velocity and sound velocity that evolve in space are shown in Fig. 2 with different combinations of g_1 and g_2 together with the simulated result for comparison purpose, where the location of the sonic horizon r_s is the coordinate of the crossing point of the v (flow velocity) curve and the c_s (sound velocity) curve, and the sonic horizon exists within an oscillation period of $\frac{\dot{\rho}(t)}{\rho(t)}$. It varies with time in the time interval of $\dot{\rho}(t) > 0$ and disappears in the

© Author(s) 2019

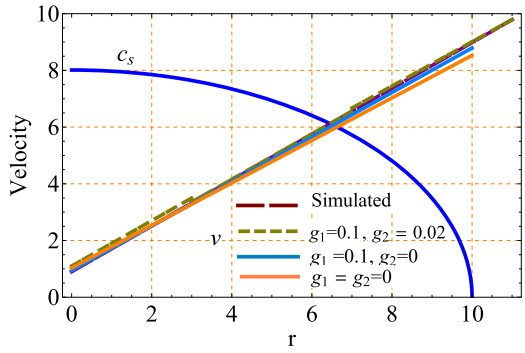

FIG. 2. System flow velocity $v(r)$ and sound speed $c_s(r)$ vs r at the timing location when distribution width σ is located at the minimum of $V(\sigma)$, based on Eqs. (12) and (13) with different combinations of g_1 and g_2 together with the simulated result for comparison purpose [in units of $(\hbar\omega/m)^{1/2}$].

time interval of $\dot{\rho}(t) < 0$. From Fig. 2, we can see that when the higher-order nonlinear effect is incorporated ($g_2 \neq 0$), the system flow velocity coincides better with that obtained from the simulated analysis.

V. CONCLUSION

In this study, the effects of higher-order nonlinear interaction are incorporated in the study of sonic horizon formation dynamics for an isotropic Bose-Einstein condensate system in harmonic trapping potential. The analytical formulation for the occurrence of the sonic black hole horizon is derived based on the three-dimensional Gross-Pitaevskii equation utilizing the modified variational method. Furthermore, we graphically demonstrate the effects of various order nonlinear interaction contributions which affect the oscillation mode region of the system distribution width $\rho(t)$. We identify the stabilization and metastable widening effects of the higher-order nonlinear interaction in the "potential" curve of the system distribution width parameter $\rho(t)$. The theoretical results derived here can be used to guide experimental investigation of sonic black hole dynamics in the Bose-Einstein condensate incorporating the higher-order nonlinear interaction effects.

ACKNOWLEDGMENTS

This work was supported by the National Natural Science Foundation (NSF) of China under Grant Nos. 11847093 and 11547024 and the Postgraduate Research and Practice Innovation Program of Jiangsu Province under Grant No. KYCX19_1681.

REFERENCES

[1] M. Belic and W. P. Zhong, Phys. Rev. A **79**, 023804 (2009).
[2] D. Tanese, H. Flayac, D. Solnyshkov *et al.*, Nat. Commun. **4**, 1749 (2013).
[3] Y. Wang, Y. Yang, S. Q. He, and W. Wang, AIP Adv. **7**, 105209 (2017).
[4] L. Dong, F. Ye, J. Wang *et al.*, Physica D **194**, 219–226 (2004).
[5] A. Minzoni, N. F. Smyth, Z. Xu *et al.*, Phys. Rev. A **79**, 063808 (2009).
[6] K. Kim and Y. K. Cho, Opto-Electron. Rev. **18**(4), 388–393 (2010).
[7] W. G. Unruh, Phys. Rev. Lett. **46**, 1351 (1981).
[8] C. Barcelo, S. Liberati, and M. Visser, Living Rev. Relativ. **8**, 12 (2005).
[9] G. Modugno, Nat. Phys. **10**, 793–794 (2014).
[10] Y. Wang and S. Y. Zhou, Chin. Phys. B **27**, 100312 (2018).
[11] Q. Chen, J. Stajic, S. Tan *et al.*, Phys. Rep. **412**, 1–88 (2004).
[12] P. R. Anderson, R. Balbinot, A. Fabbri *et al.*, Phys. Rev. D **90**, 104044 (2014).
[13] C. Lee, Phys. Rev. Lett. **93**, 120406 (2004).
[14] J. Denschlag *et al.*, Science **287**, 97–101 (2000).
[15] P. Engels and C. Atherton, Phys. Rev. Lett. **99**, 160405 (2007).
[16] W. Wen and G. X. Huang, Phys. Rev. A **79**, 023605 (2009).
[17] Y. Wang and Y. Zhou, AIP Adv. **4**, 067131 (2014).
[18] Y. Wang, W. Wang, and S. Y. Zhou, Commun. Theor. Phys. **68**, 623 (2017).
[19] W. Qi, Z. X. Liang, and Z. D. Zhang, J. Phys. B: At., Mol. Opt. Phys. **46**, 175301 (2013).
[20] E. Zaremba, Phys. Rev. A **57**, 518 (1997).
[21] Y. Kurita and T. Morinari, Phys. Rev. A **76**, 053603 (2007).

© Author(s) 2019